

# Metric formalism for precision assessment in non-Hermitian systems

Javid Naikoo,<sup>1,\*</sup> Ravindra W. Chhajlany,<sup>1</sup> Jan Kołodzyński,<sup>2,3</sup> and Adam Miranowicz<sup>1</sup>

<sup>1</sup>*Institute of Spintronics and Quantum Information, Faculty of Physics and Astronomy, Adam Mickiewicz University, 61-614 Poznań, Poland*

<sup>2</sup>*Institute of Physics, Polish Academy of Sciences, Aleja Lotników 32/46, 02-668 Warsaw, Poland*

<sup>3</sup>*Centre of New Technologies, University of Warsaw, Banacha 2c, 02-097 Warszawa, Poland*

(Dated: July 1, 2025)

Enhancing measurement precision in quantum systems is vital for advancing technologies like quantum sensing and communication. Traditionally, quantum Fisher information (QFI) has been the key tool in determining precision limits within Hermitian quantum systems. However, recent research has expanded to non-Hermitian systems exhibiting real spectra. This study investigates various interpretations of non-Hermitian quantum dynamics such as the normalization and metric approaches. We demonstrate that owing to distinct types of dynamic behaviour, QFI expressions vary significantly depending on the formalism. In particular, the normalization formalism overestimates the enhancement and/or revivals in QFI, effectively post-selecting the most optimistic case of the evolution, which may give an overly favourable impression of the sensitivity and accuracy of quantum measurements. The metric-based interpretation maintains consistency with a Hermitian-like structure, offering a more stable and conservative assessment of measurement precision. This approach provides a more natural representation of the system's evolution, enabling a more accurate assessment of quantum measurement sensitivity without the need for post-selection. We support our claims by focussing on QFI dynamics for a qubit system, while advocating the metric interpretation as a more reliable guide for quantum metrology despite presenting both approaches as valid and complementary ways of understanding non-Hermitian dynamics.

## I. INTRODUCTION

Quantum Fisher information (QFI) is a fundamental concept in quantum metrology that quantifies the amount of information a quantum state encodes about unknown parameters. It serves as a crucial tool for assessing the precision limits of parameter estimation by providing ultimate precision bound known as the quantum Cramér–Rao bound [1–3]. Mathematically, QFI is derived from the symmetric logarithmic derivative [4], which characterizes how the quantum state evolves with respect to small changes in the parameter of interest [5, 6]. QFI has been applied to determine limits on the optimal estimation of different quantities, such as phases [7–16], temperature [17–21], magnetic fields [22–26], squeezing parameters [27, 28], and so on.

Beyond its role in parameter estimation, QFI has emerged as a versatile tool in the analysis of quantum states and dynamics. It has been extensively used to characterize entanglement [29, 30], quantifying non-Markovianity [31], understanding quantum speed limits [32], the quantum Zeno effect [33, 34] and macroscopic quantum phenomena [35].

Recently, interest has shifted towards non-Hermitian systems, particularly those exhibiting parity-time ( $\mathcal{PT}$ ) symmetry, where unusual physical properties emerge. These systems, unlike Hermitian ones, can display real eigenvalue spectra under specific conditions, despite not conserving probability [5]. A notable feature of these systems is the presence of exceptional points, which are singularities in parameter space where two or more eigenvalues and their corresponding eigenvectors coalesce. Unlike conventional Hermitian systems, where eigenvalues remain distinct under small perturbations, the emergence of exceptional points in non-Hermitian dynam-

ics leads to a breakdown of the usual eigenvector orthogonality and introduces striking physical consequences [36–39].

While traditional quantum metrology has largely focused on Hermitian systems [40], the exploration of non-Hermitian systems has opened new pathways for developing more sensitive quantum sensors. Recent studies have demonstrated that  $\mathcal{PT}$ -symmetric quantum sensors, which operate near exceptional points, can achieve enhanced precision in parameter estimation [41, 42]. These systems are particularly interesting because they provide novel mechanisms to surpass classical limits, especially in noisy environments [43]. However, such enhancement in precision becomes dubious in regimes where quantum noise becomes significant [44–48].

The QFI in Hermitian systems is calculated with respect to the system state given by a valid density matrix that satisfies the important requirement of probability conservation. In contrast, non-Hermitian systems introduce several complexities. The eigenvalues of non-Hermitian Hamiltonians are generally complex, and the eigenstates may lose orthogonality, necessitating the introduction of a biorthogonal framework where right and left eigenstates are treated on an equal footing [49, 50]. Therefore, in such systems, QFI cannot be straightforwardly calculated using the traditional Hermitian formalism. The proper formalism of dealing with non-Hermitian systems with real spectrum involves introducing a metric formalism that adjusts the inner product structure of the Hilbert space, leading to physically meaningful probability conserving dynamics [51]. This adjustment is necessary, as the non-Hermiticity modifies how quantum probabilities and overlaps are measured in these systems.

Contemporary research in non-Hermitian quantum metrology have also revealed new pathways for enhanced sensitivity particularly by leveraging *postselection* techniques to engineer effective non-Hermitian dynamics within a larger Hermitian framework [52–55]. While such methods can significantly amplify parameter sensitivity, they also introduce criti-

\* javid.naikoo@amu.edu.pl

cal considerations regarding the trade-off between QFI and the probability of successful postselection [56, 57]. Since postselection inherently discards a fraction of experimental outcomes, the effective metrological advantage must be assessed in terms of the total Fisher information per experimental run, rather than the raw QFI of the selected subensemble. Consequently, the widespread practice of wavefunction normalization after non-unitary evolution may lead to an overestimation of QFI by keeping only the most favorable trajectories, thereby ignoring the total statistical cost of the full process. These observations underscore the importance of careful accounting of probability conservation in assessing the metrological potential of non-Hermitian systems, thereby ensuring that reported enhancements translate into tangible experimental advantages.

The current work demonstrates that a more effective approach to non-Hermitian quantum metrology is to interpret non-Hermitian dynamics as Hermitian dynamics with a modified metric. This allows for the application of standard tools of quantum metrology for Hermitian systems, providing a more consistent and physically meaningful framework for parameter estimation in presence of a non-Hermitian Hamiltonian with real spectrum. We also compare this approach with the no-jump evolution, where the state is normalized at each time step, and further analyze the results obtained using the full master equation. These comparisons elucidate the advantages and limitations of different methodologies in non-Hermitian quantum metrology and offer insights into optimizing estimation strategies.

This paper is organized as follows. Section III examines various approaches to quantum dynamics in the presence of a non-Hermitian Hamiltonian. Section IV discusses QFI in non-Hermitian systems, emphasizing the advantages of the metric formalism for parameter estimation. In particular, we explore how both Hamiltonian and state parameters can be inferred directly from the non-Hermitian Hamiltonian and the Schrödinger equation. Section V investigates two distinct physical scenarios in which a qubit undergoes open system dynamics, illustrating different methods for estimating state parameters by computing QFI and comparing their effectiveness. Finally, Sec. VI summarizes our findings.

## II. MOTIVATION

Quantum metrology aims to determine parameters with the highest possible precision, leveraging quantum effects to enhance sensitivity. In conventional quantum mechanics, metrology is well understood for systems governed by *Hermitian* Hamiltonians with *real* eigenvalues, which form the region  $\Omega_{\text{H}}^{\text{R}}$  in the parameter space of  $H$ , where

$$H = H^\dagger. \quad (1)$$

For such systems, unitary evolution ensures that well-established metrological tools, such as the QFI, provide a reliable measure of estimation precision.

Non-Hermitian Hamiltonians, where  $H \neq H^\dagger$ , appear naturally in open quantum systems and effective descriptions of

dissipation. In the regime where at least one eigenvalue becomes *complex*, the system belongs to the region  $\Omega_{\text{NH}}^{\text{C}}$ , defined by

$$\exists \lambda_i \notin \mathbb{R}, \quad \text{where} \quad H\psi_i = \lambda_i\psi_i. \quad (2)$$

In this case, the system evolution is inherently non-unitary in the standard Hilbert space, and metrological studies typically rely on quantum master equation approaches.

An intermediate regime,  $\Omega_{\text{NH}}^{\text{R}}$ , consists of non-Hermitian Hamiltonians that nevertheless have entirely *real* eigenvalues:

$$H \neq H^\dagger, \quad \lambda_i \in \mathbb{R} \quad \forall i. \quad (3)$$

Here, a suitable choice of an inner-product structure, often referred to as a “metric” formalism, allows the system to retain unitary-like evolution under a redefined notion of unitarity. Specifically, there exists a positive-definite operator  $\eta$  (the metric) such that the Hamiltonian is quasi-Hermitian

$$H \in \Omega_{\text{NH}}^{\text{R}} \Leftrightarrow \exists \eta > 0 \text{ s.t. } H^\dagger = \eta H \eta^{-1} \quad (4)$$

Note that as  $\Omega_{\text{H}}^{\text{R}} \subset \Omega_{\text{NH}}^{\text{R}}$ , the Hermitian case corresponds to the special situation when  $\eta = \mathbb{1}$ . The qualitative structure of these regions in parameter space is illustrated in Fig. 1, which shows how the system transitions across  $\Omega_{\text{H}}^{\text{R}}$ ,  $\Omega_{\text{NH}}^{\text{R}}$ , and  $\Omega_{\text{NH}}^{\text{C}}$  for a representative two-level Hamiltonian.

In this work, we adopt the existing metric formalism to demonstrate the correct approach to quantum metrology in  $\Omega_{\text{NH}}^{\text{R}}$ . Rather than claiming enhanced precision or a metrological advantage, we show how standard quantum metrological concepts should be correctly adapted within this formalism. Our results provide a well-founded framework for analyzing parameter estimation in this regime, ensuring consistency with the broader principles of quantum mechanics.

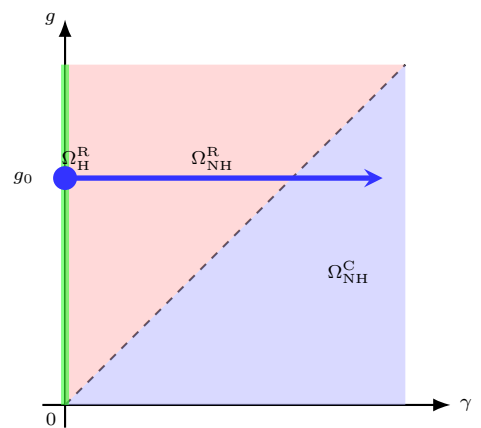


FIG. 1. **Different possible regions in the parameter space** of

a specific Hamiltonian  $H = \begin{bmatrix} -i\gamma & g \\ g & i\gamma \end{bmatrix}$ , illustrating the transition along the slice  $g = g_0$ . The system moves from  $\Omega_{\text{H}}^{\text{R}}$  at  $\gamma = 0$  to  $\Omega_{\text{NH}}^{\text{R}}$  for  $0 < \gamma < g$ , and then to  $\Omega_{\text{NH}}^{\text{C}}$  for  $0 < g < \gamma$ . Here,  $\Omega_{\text{H}}^{\text{R}}$  and  $\Omega_{\text{NH}}^{\text{C}}$  denote regions in the parameter space of  $H$  corresponding to Hermitian Hamiltonians with real eigenvalues and non-Hermitian Hamiltonians with complex eigenvalues, respectively, while  $\Omega_{\text{NH}}^{\text{R}}$  refers to the intermediate region of non-Hermitian Hamiltonians that still possess real eigenvalues.

### III. APPROACHES TO NON-HERMITIAN DYNAMICS

This section introduces key formalisms—the metric formalism, the normalization method, and the master equation approach—highlighting their roles in governing quantum state evolution. These frameworks will later be used to analyze the precision of estimating unknown state parameters and to examine the resulting differences in behavior of the precision across the formalisms.

#### A. Metric framework

Throughout the rest of this work, we use a tilde ( $\tilde{\cdot}$ ) to denote operators or matrices in the non-Hermitian frame, i.e., those defined with respect to the standard inner product. Corresponding quantities in the Hermitian (or metric-transformed) frame, where the dynamics is unitarily equivalent under the metric operator  $\eta$ , are written without the tilde.

Consider a system  $\mathcal{S}_{\text{NH}}$  described by a non-Hermitian Hamiltonian  $\tilde{H} : \tilde{\mathcal{H}} \rightarrow \tilde{\mathcal{H}}$ . The non-Hermiticity implies  $\tilde{H}^\dagger \neq \tilde{H}$  where the adjoint  $^\dagger$  is defined by the relation  $\langle \tilde{H}^\dagger \tilde{\psi} | \tilde{\psi} \rangle = \langle \tilde{\psi} | \tilde{H} \tilde{\psi} \rangle$  and  $\langle \tilde{\psi} | \tilde{\phi} \rangle$  is the *standard* inner product. In particular, if  $\tilde{H}$  satisfies  $\tilde{H}^\dagger = \eta \tilde{H} \eta^{-1}$  for a positive-definite operator  $\eta > 0$  then it is called as a pseudo-Hermitian Hamiltonian and this condition is necessary and sufficient for  $\tilde{H}$  to have real eigenvalues [58]. As discussed earlier, such a non-Hermitian Hamiltonian belongs to the regime  $\Omega_{\text{NH}}^{\text{R}}$ , and admits a similarity transformation that renders it Hermitian with respect to a modified inner product.

Let  $\mathcal{H}_\eta$  be the space  $\tilde{\mathcal{H}}$  but equipped now with the metric defined by the positive-definite operator  $\eta$  introduced above, i.e. for any  $\tilde{\psi}, \tilde{\phi} \in \mathcal{H}_\eta$  their inner product reads  $\langle \tilde{\psi} | \tilde{\phi} \rangle_\eta := \langle \tilde{\psi} | \eta | \tilde{\phi} \rangle$ . Then, by defining a map, which can be interpreted as a vielbein [59, 60],  $\mathcal{E} : \mathcal{H}_\eta \rightarrow \mathcal{H}$  such that  $|\mathcal{E}\tilde{\psi}\rangle = \sqrt{\eta}|\tilde{\psi}\rangle \in \mathcal{H}$  for any  $\tilde{\psi} \in \mathcal{H}_\eta$  and its unique inverse  $\mathcal{E}^{-1} : \mathcal{H} \rightarrow \mathcal{H}_\eta$  with  $|\mathcal{E}^{-1}\psi\rangle = \sqrt{\eta^{-1}}|\psi\rangle \in \mathcal{H}_\eta$  for any  $\psi \in \mathcal{H}$ , one obtains a Hilbert space  $\mathcal{H}$  that is equipped with a standard inner product. In particular, for any  $\tilde{\psi}, \tilde{\phi} \in \mathcal{H}_\eta$  one may identify  $\psi = \mathcal{E}\tilde{\psi}, \phi = \mathcal{E}\tilde{\phi} \in \mathcal{H}$  such that

$$\begin{aligned} \langle \tilde{\psi} | \tilde{\phi} \rangle_\eta &= \langle \tilde{\psi} | \eta | \tilde{\phi} \rangle = \langle \mathcal{E}^{-1}\psi | \eta | \mathcal{E}^{-1}\phi \rangle = \langle \psi | (\mathcal{E}^{-1})^\dagger \eta \mathcal{E}^{-1} | \phi \rangle \\ &= \langle \psi | (\sqrt{\eta^{-1}})^\dagger \eta \sqrt{\eta^{-1}} | \phi \rangle = \langle \psi | \phi \rangle, \end{aligned} \quad (5)$$

from which it also follows that  $\mathcal{E} = \mathcal{E}^\dagger$  and  $\mathcal{E}^\dagger \mathcal{E} = \eta$ .

Moreover, it is now possible to identify the Hermitian counterpart of the system,  $\mathcal{S}_{\text{H}}$ , in the Hilbert space  $\mathcal{H}$  by identifying the equivalent Schrödinger equation governing the time evolution, i.e.:

$$\begin{aligned} i \frac{d}{dt} |\tilde{\psi}(t)\rangle &= \tilde{H} |\tilde{\psi}(t)\rangle && \text{non-Hermitian system, } \mathcal{S}_{\text{NH}} \\ i \frac{d}{dt} |\psi(t)\rangle &= H |\psi(t)\rangle && \text{its Hermitized counterpart, } \mathcal{S}_{\text{H}} \end{aligned} \quad (6)$$

where with any  $\tilde{\psi}(t) \in \mathcal{H}_\eta$  one associates  $\psi(t) = \mathcal{E}\tilde{\psi}(t) \in \mathcal{H}$  whose dynamics is generated by a *Hermitian* Hamilto-

nian [59]:

$$H = \mathcal{E} \tilde{H} \mathcal{E}^{-1} + i(\partial_t \mathcal{E}) \mathcal{E}^{-1}. \quad (7)$$

As a result, allowing the metric  $\eta$  (or equivalently the vielbein  $\mathcal{E}$ ) to be time-dependent, the original Hamiltonian,  $\tilde{H}$ , generates unitary dynamics in  $\mathcal{H}_\eta$  only if the metric operator  $\eta$  satisfies the general equation of motion [59, 61]:

$$i \frac{d}{dt} \eta(t) = \tilde{H}^\dagger \eta(t) - \eta(t) \tilde{H}. \quad (8)$$

This starkly contrasts the evolution of  $\psi(t)$  in  $\mathcal{H}$ , which is guaranteed to be unitary by the Hermiticity of  $H$  in Eq. (7). For consistency, note that in the special trivial case of  $\tilde{H} = \tilde{H}^\dagger \in \Omega_{\text{H}}^{\text{R}}$ , marked in Fig. 1,  $\eta = \mathbb{1}$  and  $\mathcal{E}$  becomes a (time-independent) identity map, so that consistently  $H = \tilde{H}$  in Eq. (7) with  $\mathcal{H} \equiv \mathcal{H}_\eta$ , whereas the r.h.s. of Eq. (8) vanishes.

Similarly, for any observable  $\tilde{A} : \mathcal{H}_\eta \rightarrow \mathcal{H}_\eta$ , which by definition is Hermitian (no matter the metric  $\eta$ ), we may identify its equivalent  $A$  in the Hilbert space  $\mathcal{H}$  by considering any  $\tilde{\psi} \in \mathcal{H}_\eta$  that maps onto  $\psi = \mathcal{E}\tilde{\psi} \in \mathcal{H}$ , and the corresponding expectation value:

$$\begin{aligned} \frac{\langle \tilde{\psi} | \tilde{A} | \tilde{\psi} \rangle_\eta}{\langle \tilde{\psi} | \tilde{\psi} \rangle_\eta} &= \frac{\langle \tilde{\psi} | \eta \tilde{A} | \tilde{\psi} \rangle}{\langle \tilde{\psi} | \eta | \tilde{\psi} \rangle} = \frac{\langle \tilde{\psi} | \mathcal{E}^\dagger \mathcal{E} \tilde{A} | \tilde{\psi} \rangle}{\langle \tilde{\psi} | \mathcal{E}^\dagger \mathcal{E} | \tilde{\psi} \rangle} = \frac{\langle \tilde{\psi} | \mathcal{E}^\dagger \mathcal{E} \tilde{A} \mathcal{E}^{-1} \mathcal{E} | \tilde{\psi} \rangle}{\langle \tilde{\psi} | \mathcal{E}^\dagger \mathcal{E} | \tilde{\psi} \rangle} \\ &= \frac{\langle \mathcal{E}\tilde{\psi} | \mathcal{E} \tilde{A} \mathcal{E}^{-1} | \mathcal{E}\tilde{\psi} \rangle}{\langle \mathcal{E}\tilde{\psi} | \mathcal{E}\tilde{\psi} \rangle} = \frac{\langle \psi | A | \psi \rangle}{\langle \psi | \psi \rangle}, \end{aligned} \quad (9)$$

which yields

$$A = \mathcal{E} \tilde{A} \mathcal{E}^{-1} : \mathcal{H} \rightarrow \mathcal{H}. \quad (10)$$

In the converse direction, Eq. (10) should also be viewed as a recipe for obtaining the Hermitian observables  $A$  acting in  $\mathcal{H}_\eta$  from their counterpart  $A$  in  $\mathcal{H}$ . For instance, the generalised Pauli operator  $\tilde{\sigma} : \mathcal{H} \rightarrow \mathcal{H}$  is the Hermitised counterpart of operator  $\tilde{\sigma} = \mathcal{E}^{-1} \tilde{\sigma} \mathcal{E}$  acting in metric space  $\mathcal{H}_\eta$ . More importantly, the energy observable acting in  $\mathcal{H}_\eta$  associated with the Hermitised Hamiltonian (7) is given by  $\tilde{H}_E = \mathcal{E}^{-1} H \mathcal{E}$ , which is not the same as  $\tilde{H}$  appearing in Eq. (6), unless  $\mathcal{E}$  is time-independent [61].

#### B. Time-dependent normalization approach

When non-Hermitian Hamiltonians are applied within the framework of the Schrödinger equation, they typically produce a time-dependent state that does not fulfill the essential criterion of a density matrix, namely that its trace must equal one. Consequently, the resulting state is not physically valid, as the trace condition is crucial for ensuring the proper normalization of probabilities in quantum mechanics. A common remedy for this issue involves normalizing the state by dividing it by its trace, thereby restoring the trace to unity

$$\rho_{\text{norm}}(t) = \frac{e^{-i\tilde{H}t} \rho_0 e^{i\tilde{H}t}}{\text{Tr}[e^{-i\tilde{H}t} \rho_0 e^{i\tilde{H}t}]}, \quad (11)$$

The normalized physical quantities are then computed as:

$$\langle A(t) \rangle_{\text{norm}} = \frac{\langle \tilde{\psi}(t) | A | \tilde{\psi}(t) \rangle}{\langle \tilde{\psi}(t) | \tilde{\psi}(t) \rangle} = \frac{\text{Tr}[\tilde{\rho}(t)A]}{\text{Tr}[\tilde{\rho}(t)]} = \text{Tr}[\rho_{\text{norm}}(t)A]. \quad (12)$$

Interestingly,  $\rho_{\text{norm}}(t)$  satisfies the following non-linear equation of motion [62]

$$\frac{d}{dt}\rho_{\text{norm}}(t) = -i[\tilde{H}_R, \rho_{\text{norm}}(t)] - \left( \{\tilde{H}_I, \rho_{\text{norm}}(t)\} - 2\text{Tr}[\rho_{\text{norm}}(t)\tilde{H}_I]\rho_{\text{norm}}(t) \right), \quad (13)$$

where  $\tilde{H}_R$  and  $\tilde{H}_I$  are the real and imaginary parts of  $\tilde{H}$ , and  $\{\cdot, \cdot\}$  denotes the anticommutator.

The normalization procedure is widely used in systems governed by non-Hermitian effective Hamiltonians. However, despite its mathematical convenience, this approach warrants careful examination, as it may obscure or distort the true dynamics and physical interpretation of the system's evolution as it leads to the violation of canonical commutation relations [63, 64].

### C. Conditional non-Hermitian dynamics in master equations

Dissipation is a key source of non-Hermiticity in quantum systems. Under the Born-Markov approximation, open quantum systems are governed by the master equation in the Lindblad form:

$$\dot{\rho}_{\text{me}}(t) = -i[H, \rho_{\text{me}}(t)] + \sum_{\ell} \left( \Gamma_{\ell} \rho_{\text{me}}(t) \Gamma_{\ell}^{\dagger} - \frac{1}{2} \{ \rho_{\text{me}}(t), \Gamma_{\ell}^{\dagger} \Gamma_{\ell} \} \right), \quad (14)$$

where  $\rho_{\text{me}}$  is the system's density matrix,  $H$  is the Hamiltonian, and  $\Gamma_j$  are Lindblad operators describing the system-environment interaction. The expectation value of an observable  $A$  is given by  $\langle A \rangle_{\text{me}} = \text{Tr}(\rho_{\text{me}}A)$ . Directly solving the master equation is computationally intensive. Instead, the quantum trajectory method tracks individual quantum states evolving under an effective non-Hermitian Hamiltonian

$$H_{\text{eff}} = H - \frac{i}{2} \sum_{\ell} \Gamma_{\ell}^{\dagger} \Gamma_{\ell}, \quad (15)$$

punctuated by random quantum jumps. Averaging over the ensemble of pure states reproduces the density matrix  $\rho_{\text{me}}$ , and observables can be calculated accordingly.

The conditional evolution under the assumption that “no jump” has occurred is described by

$$\dot{\rho}_{\text{nj}}(t) = -i(H_{\text{eff}}\rho_{\text{nj}}(t) - \rho_{\text{nj}}(t)H_{\text{eff}}^{\dagger}), \quad (16)$$

neglecting the quantum jump term. The corresponding expectation value is given by

$$\langle A(t) \rangle_{\text{nj}} = \frac{\text{Tr}[\rho_{\text{nj}}(t)A]}{\text{Tr}[\rho_{\text{nj}}(t)]}. \quad (17)$$

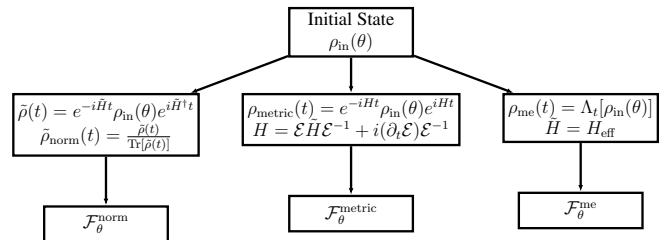


FIG. 2. **Different ways of evaluating the QFI** given an initial state  $\rho_{\text{in}}(\theta)$  and a non-Hermitian Hamiltonian  $\tilde{H}$  generating the evolution. The approaches include: (1) normalizing the non-Hermitian state  $\tilde{\rho}(t)$  by its trace at each time step, (2) transforming the state into a metric space with a modified inner product, (3) solving the full master equation to incorporate both coherent evolution and dissipation in open systems. The reason we compare these approaches is that they all describe probability conserving dynamics.

It should be emphasized that Eqs. (16) and (17) correspond respectively to Eqs. (11) and (12) discussed in normalization approach above, wherein one considers only those experimental realizations in which no quantum jumps occur. This *post-selection* is inherently optimistic because it neglects the effects of quantum jumps, which typically induce decoherence and diminish the precision of parameter estimation. Despite its theoretical appeal, post-selected quantum metrology inherently discards a large fraction of data, rendering any gain in QFI ineffective due to the low success probability [57].

These different methods generally lead to distinct physical predictions. For example, in the quantum brachistochrone problem, normalization methods can predict arbitrarily fast quantum evolution using  $\mathcal{PT}$ -symmetry [65]. However, studies using the metric formalism show that faster unitary evolution is not achievable with non-Hermitian Hamiltonians compared to Hermitian ones [66]. Similarly, the metric formalism predicts non-zero defect densities near exceptional points, which contrasts with results from simple norm division methods [67]. Further, claims of no-go theorem violations in non-Hermitian systems may stem from incorrect operator definitions [64].

Alternatively, another fully quantum approach based on the Heisenberg-Langevin (HL) equations of motion could be considered. This method has garnered increasing interest recently, especially in analyzing quantum exceptional points of Gaussian fields [see Refs. [47, 68–72]]. Although the HL approach yields predictions consistent with the master equation approach, it is not described in detail here. For a detailed comparison of the normalization and HL approaches for Gaussian processes, see Ref. [69].

## IV. QFI FOR NON-HERMITIAN HAMILTONIANS

In parameter estimation, the goal is to determine an estimator  $\hat{\theta}$  that maps measurement outcomes  $\chi$  to a parameter space. In classical estimation theory, an estimator is considered optimal if it achieves the Cramér-Rao bound  $\delta^2\theta \geq 1/\nu F_{\theta}$ , where  $\delta^2\theta$  denotes the mean square error,  $\nu$  is the number of measurements, and  $F_{\theta}$  is the Fisher information

given by [73]:

$$\begin{aligned} F_\theta &= \int dx p(x|\theta) \left( \frac{\partial \ln p(x|\theta)}{\partial \theta} \right)^2, \\ &= \int \frac{1}{p(x|\theta)} \left( \frac{\partial p(x|\theta)}{\partial \theta} \right)^2 dx. \end{aligned} \quad (18)$$

For unbiased estimators, the mean square error is equivalent to the variance  $\text{Var}(\theta) = E_\theta[\hat{\theta}^2] - E_\theta[\hat{\theta}]^2$ .

In quantum parameter estimation, one deals with a family of quantum states  $\rho_\theta$  depending on unknown parameter  $\theta$ . The parameter  $\theta$  is inferred through measurements on  $\rho_\theta$  and the probability distribution of outcomes is expressed as  $p(x|\theta) = \text{Tr}[\Pi_x \rho_\theta]$ , where  $\{\Pi_x\}$  are the elements of a POVM with  $\int dx \Pi_x = \mathbb{1}$ . The classical Fisher information in this context is [5]:

$$\begin{aligned} F_\theta &= \int dx \frac{\text{Tr}[\Pi_x \partial_\theta \rho_\theta]^2}{\text{Tr}[\rho_\theta \Pi_x]}, \\ &= \int dx \frac{[\text{Re}(\text{Tr}[\rho_\theta \Pi_x L_\theta])]^2}{\text{Tr}[\rho_\theta \Pi_x]}, \end{aligned} \quad (19)$$

where  $L_\theta$  is the symmetric logarithmic derivative and is defined implicitly as  $\partial_\theta \rho_\theta = (L_\theta \rho_\theta + \rho_\theta L_\theta)/2$ . Maximizing this bound over all possible quantum measurements (POVMs) determines the ultimate attainable limit of precision in terms of the QFI  $\mathcal{F}_\theta$  such that

$$F_\theta \leq \mathcal{F}_\theta = \text{Tr}[\rho_\theta L_\theta^2]. \quad (20)$$

In the more general setting of multiparameter estimation, Eq. (20) generalises to a matrix inequality that, however, is no longer guaranteed to be saturable despite maintaining its validity [74]. For a given set of parameters  $\theta = \{\theta_\ell\}_{\ell=0}^n$ , each entry of the QFI matrix of size  $n \times n$  is then indexed by parameters from the set, and for any  $\theta_i, \theta_j \in \theta$  it reads

$$\mathcal{F}_{\theta_i, \theta_j} = \frac{1}{2} \text{Tr}(\rho_\theta \{\mathcal{L}_{\theta_i}, \mathcal{L}_{\theta_j}\}). \quad (21)$$

where  $\{\cdot, \cdot\}$  denotes again the anticommutator.

For instance, in the special case of a *mixed qubit state*  $\rho_\theta$ , each entry of the QFI matrix is given by the following formula [75, 76]:

$$\begin{aligned} \mathcal{F}_{\theta_i, \theta_j} &= \text{Tr}[(\partial_{\theta_i} \rho_\theta)(\partial_{\theta_j} \rho_\theta)] \\ &+ \frac{1}{\det(\rho_\theta)} \text{Tr}[\rho_\theta (\partial_{\theta_i} \rho_\theta) \rho_\theta (\partial_{\theta_j} \rho_\theta)]. \end{aligned} \quad (22)$$

While the QFI is well-defined for Hermitian systems, extending its formulation to non-Hermitian dynamics introduces challenges. Non-Hermitian Hamiltonians induce non-unitary evolution, yield complex eigenvalues, and break probability conservation, thereby complicating the direct application of standard QFI formulas. As discussed in Sec. III and illustrated in Fig. 2, several possibilities exist to tackle these issues, including wavefunction normalization, the metric formalism, and the master equation approach. Each method has

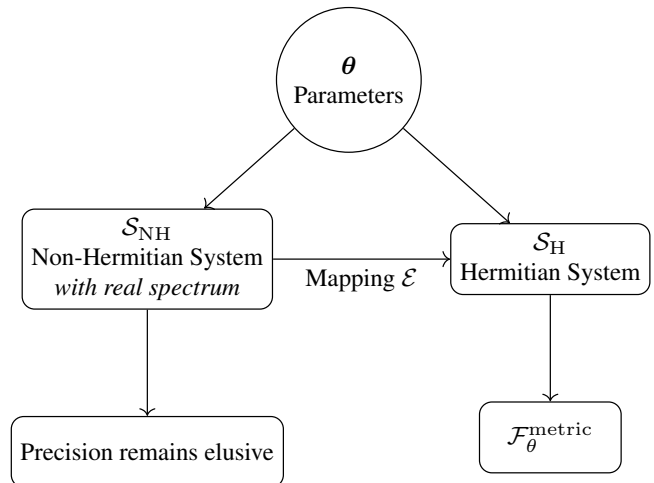


FIG. 3. A set of parameters  $\theta$  is associated with non-Hermitian system  $\mathcal{S}_{\text{NH}}$  with *real eigenvalues*, where direct estimation of  $\theta$  is challenging. To simplify the process,  $\mathcal{S}_{\text{NH}}$  is mapped, using a proper *metric*, to a Hermitian system  $\mathcal{S}_{\text{H}}$ , which retains the *same parameters* but allows for easier inference. The estimation of  $\theta$  in metric space is then achieved using the conventional QFI formalism for Hermitian systems.

distinct implications for the computation of QFI, and in the following we explore how the QFI behaves depending on the approach undertaken.

However, as each of the approaches summarised in Fig. 2 leads to different dynamics given the non-Hermitian  $\tilde{H}$  considered, it would be inappropriate to compare them by considering metrology scenarios in which the parameters  $\theta$  are encoded by the non-Hermitian Hamiltonian itself, i.e.  $\tilde{H}(\theta)$ . Each approach would then yield different  $\theta$ -encoding mechanism, making their corresponding QFIs incomparable. That is why, when dealing with particular physical system in Sec. V we assume the parameters to be encoded onto the initial state  $\rho_{\text{in}}(\theta)$ , as emphasised in Fig. 2. Each approach determines then the  $\theta$ -independent evolution over time  $t$  onto the final state  $\rho(t)$ , whose QFI quantifies then the sensitivity to changes of  $\theta$  in the initial state common to all three methods.

Nonetheless, in this work we advocate particularly for the metric formalism summarised schematically in Fig. 3. In particular, we argue that the QFI for a non-Hermitian system  $\mathcal{S}_{\text{NH}}$  with real spectrum should be evaluated by reformulating the dynamics within the Hermitian frame  $\mathcal{S}_{\text{H}}$  introduced in Eq. (6). By transforming to an equivalent Hermitian frame, one can directly apply the well-established QFI formula in Eq. (21) used for Hermitian systems. We illustrate this with the following example of a general  $\tilde{H}(\theta)$  with  $\theta = \{r, s, \tau, \phi\}$  encoding these parameters onto a qubit.

#### A. General $2 \times 2$ non-Hermitian Hamiltonian

Consider a non-Hermitian system  $\mathcal{S}_{\text{nh}}(r, s, \tau, \phi)$  characterised by real parameters  $r, s, \tau$ , and  $\phi$ , through the following

non-Hermitian Hamiltonian [77]

$$\tilde{H} = \begin{pmatrix} r + \tau C_\phi - i s S_\phi & i s C_\phi + \tau S_\phi \\ i s C_\phi + \tau S_\phi & r - \tau C_\phi + i s S_\phi \end{pmatrix}, \quad (23)$$

where  $C_\phi = \cos(\phi)$  and  $S_\phi = \sin(\phi)$ . The eigenvalues of  $\tilde{H}$  are real for  $|s| \leq |\tau|$ . The metric operator and its square root are given by

$$\eta = \begin{pmatrix} \sec(\alpha) & i \tan(\alpha) \\ -i \tan(\alpha) & \sec(\alpha) \end{pmatrix},$$

$$\mathcal{E} = \sqrt{\eta} = \begin{pmatrix} r_+ & -i r_- \\ i r_- & r_+ \end{pmatrix}, \quad (24)$$

with  $r_\pm := \frac{1}{2} \left( \sqrt{\sec(\alpha) - \tan(\alpha)} \pm \sqrt{\sec(\alpha) + \tan(\alpha)} \right)$ . The same system can be described by an equivalent Hermitian  $S_{\text{herm}}(r, s, \tau, \phi)$  with Hermitian Hamiltonian

$$H = \begin{pmatrix} r + \sqrt{\tau^2 - s^2} C_\phi & \sqrt{\tau^2 - s^2} S_\phi \\ \sqrt{\tau^2 - s^2} S_\phi & r - \sqrt{\tau^2 - s^2} C_\phi \end{pmatrix}. \quad (25)$$

Since the new system depends on the same set of parameters  $r, s, \tau$  and  $\phi$ , we choose to estimate them in the Hermitian frame instead. For this, let us consider the following initial state with real parameters  $\theta$  and  $x$ :

$$\rho_{\text{in}} = \begin{pmatrix} 1 - \theta & x \\ x & \theta \end{pmatrix}, \quad (26)$$

where  $x \in [0, \sqrt{\theta(1-\theta)}]$ . Under the time dynamics,  $\rho(t) = \exp(-iHt)\rho_{\text{in}}\exp(iHt)$ , estimating the parameters of the Hamiltonian requires calculating the QFI matrix. This can be accomplished by applying the formula in Eq. (22) for mixed qubit state, resulting in the QFI

$$\mathcal{F} = \begin{pmatrix} 0 & 0 & 0 & 0 \\ 0 & \mathcal{F}_{ss} & \mathcal{F}_{st} & \mathcal{F}_{s\phi} \\ 0 & \mathcal{F}_{ts} & \mathcal{F}_{tt} & \mathcal{F}_{t\phi} \\ 0 & \mathcal{F}_{\phi s} & \mathcal{F}_{\phi s} & \mathcal{F}_{\phi\phi} \end{pmatrix}, \quad (27)$$

where

$$\mathcal{F}_{ss} = \frac{4s^2t^2[(2\theta - 1)S_\phi + 2xC_\phi]^2}{s^2 + \tau^2},$$

$$\mathcal{F}_{s\phi} = \frac{stS_\alpha[\kappa_- S_{2\phi} + \lambda C_{2\phi}]}{\sqrt{s^2 + \tau^2}},$$

$$\mathcal{F}_{s\tau} = \frac{\tau}{s} \mathcal{F}_{ss}, \mathcal{F}_{\tau s} = \mathcal{F}_{s\tau}, \mathcal{F}_{\tau\tau} = \frac{\tau}{s} \mathcal{F}_{\tau s},$$

$$\mathcal{F}_{\tau\phi} = \frac{\tau}{s} \mathcal{F}_{s\phi}, \mathcal{F}_{\phi s} = \mathcal{F}_{s\phi}, \mathcal{F}_{\phi\tau} = \mathcal{F}_{\tau\phi},$$

$$\mathcal{F}_{\phi\phi} = \frac{1}{2} S_\alpha^2 [\kappa_- C_{2\phi} - \lambda S_{2\phi}] - \kappa_+ S_{\alpha/2}^2 (C_\alpha - 3), \quad (28)$$

where various parameters are  $\alpha = 2t\sqrt{s^2 + \tau^2}$ ,  $\kappa_\pm = ((1 - 2\theta)^2 \pm 4x^2)$  and  $\lambda = 4(2\theta - 1)x$ .

In some cases the parameters of the input state itself may be unknown, for example, the population  $\theta$  of different energy

levels or the coherence  $x$  between them. In that case, the relevant QFI matrix elements are given by

$$\mathcal{F}_{\theta\theta} = \frac{1 - 4x^2}{\theta(1-\theta) - x^2},$$

$$\mathcal{F}_{xx} = \frac{4(1-\theta)\theta}{\theta(1-\theta) - x^2},$$

$$\mathcal{F}_{\theta x} = \frac{2x(2\theta - 1)}{\theta(1-\theta) - x^2} = \mathcal{F}_{x\theta}. \quad (29)$$

The QFI matrix elements presented here, encompassing both diagonal and off-diagonal components, are essential for characterizing unknown parameters whether for both Hamiltonian and the input state. The diagonal elements capture the system's sensitivity to variations in individual parameters, thereby providing critical insights into the uncertainties linked to each parameter. In contrast, the off-diagonal elements elucidate the interdependencies between these parameters, demonstrating how fluctuations in one can significantly impact the estimation of another.

## B. Impact of quantum jumps on quantum Fisher information

In light of Sec. III C, a crucial aspect of understanding QFI in non-Hermitian metrology is assessing the impact of quantum jumps on parameter sensitivity. One way to analyze this effect is by comparing the QFI obtained from the full master equation solution with that of the no-jump evolution. To facilitate this comparison, we examine the finite-difference form of Eq. (14) for small  $dt$ , which systematically captures the influence of quantum jumps on the dynamics. Specifically, we express the evolution of the density matrix as

$$\rho_{\text{me}}(t + dt) = \rho_{\text{me}}(t) - i[H, \rho_{\text{me}}(t)]dt$$

$$+ \sum_{\ell} \left( \Gamma_{\ell} \rho_{\text{me}}(t) \Gamma_{\ell}^{\dagger} - \frac{1}{2} \{ \rho_{\text{me}}(t), \Gamma_{\ell}^{\dagger} \Gamma_{\ell} \} \right) dt$$

$$+ \mathcal{O}(dt^2)$$

$$= \rho_{\text{me}}(t) - i \left( H_{\text{eff}} \rho_{\text{me}}(t) - \rho_{\text{me}}(t) H_{\text{eff}}^{\dagger} \right) dt$$

$$+ dt \sum_{\ell} \Gamma_{\ell} \rho_{\text{me}}(t) \Gamma_{\ell}^{\dagger} + \mathcal{O}(dt^2), \quad (30)$$

where  $H_{\text{eff}}$ , the effective Hamiltonian, is given by Eq. (15).

To reformulate this evolution in a more insightful form, we define the non-unitary evolution operator

$$M_0(dt) = \mathbb{1} - i H_{\text{eff}} dt \approx e^{-i H_{\text{eff}} dt}, \quad (31)$$

which describes the no-jump evolution. Additionally, we introduce

$$M_{\ell}(dt) = \Gamma_{\ell} \sqrt{dt}, \quad (32)$$

which accounts for the effect of quantum jumps. With these definitions, Eq. (30) can be rewritten as

$$\rho_{\text{me}}(t + dt) = M_0 \rho_{\text{me}}(t) M_0^{\dagger} + \sum_{\ell > 0} M_{\ell} \rho_{\text{me}}(t) M_{\ell}^{\dagger} + \mathcal{O}(dt^2). \quad (33)$$

These operators satisfy the completeness relation

$$\sum_{\ell} M_{\ell}^{\dagger} M_{\ell} = \mathbb{1} + \mathcal{O}(dt^2), \quad (34)$$

which ensures proper normalization up to second-order corrections in  $dt$ .

This decomposition of the master equation clearly distinguishes between contributions from the no-jump evolution and quantum jumps, providing a systematic way to analyze their respective effects on QFI. Specifically, the full density matrix can be expressed as a probabilistic mixture of conditional states:

$$\rho_{\text{me}}(t+dt) = p_0(t+dt)\rho_{\text{nj}}(t+dt) + \sum_{\ell} p_{\ell}(t+dt)\rho_{\text{j}}^{(\ell)}(t+dt). \quad (35)$$

Here, the individual components are given by:

- **No-jump evolution:** The state  $\rho_{\text{nj}}(t+dt)$  corresponds to the evolution without quantum jumps, governed by the non-Hermitian effective Hamiltonian:

$$\rho_{\text{nj}}(t+dt) = \frac{M_0(dt)\rho_{\text{me}}(t)M_0^{\dagger}(dt)}{p_0(t+dt)}, \quad (36)$$

occurring with probability

$$p_0(t+dt) = \text{Tr}[M_0(dt)\rho_{\text{me}}(t)M_0^{\dagger}(dt)]. \quad (37)$$

- **Jump evolution:** The states  $\rho_{\text{j}}^{(\ell)}(t+dt)$  represent the system's evolution conditioned on the occurrence of the  $\ell$ -th quantum jump

$$\rho_{\text{j}}^{(\ell)}(t+dt) = \frac{M_{\ell}\rho_{\text{me}}(t)M_{\ell}^{\dagger}}{p_{\ell}(t+dt)}, \quad (38)$$

which occurs with probability

$$p_{\ell}(t+dt) = \text{Tr}[M_{\ell}(dt)\rho_{\text{me}}(t)M_{\ell}^{\dagger}(dt)], \quad \ell > 0. \quad (39)$$

This formulation explicitly separates the deterministic no-jump evolution from the stochastic jump-induced transitions, offering a clear framework to quantify their respective contributions to QFI. This decomposition plays a crucial role in establishing bounds on QFI, as [78]

$$\mathcal{F}_{\theta}(\rho_{\text{nj}}(t+dt)) \geq \mathcal{F}_{\theta}(\rho_{\text{me}}^{(\ell)}(t+dt)). \quad (40)$$

## V. PHYSICAL SYSTEMS

We now examine two physical scenarios to illustrate the behavior of QFI and the associated system properties. The first scenario involves a static metric operator, while the second considers a dynamic metric operator. These contrasting cases will help to highlight the differences in QFI and its implications for the system.

### A. Time-independent metric: Biorthogonal system

Consider the non-Hermitian Hamiltonian

$$\tilde{H}_1 = \begin{pmatrix} \omega_0 - i\gamma & g \\ g & \omega_0 + i\gamma \end{pmatrix}, \quad (41)$$

which represents a two-level quantum system, where the levels are coupled through a parameter  $g$ , and experience gain and loss dynamics characterized by the imaginary terms  $\pm i\gamma$ . The real part of the diagonal elements,  $\omega_0$ , represents the energy levels of the two states, while the off-diagonal coupling term  $g$  dictates the strength of interaction between the states. The imaginary parts,  $-i\gamma$  and  $+i\gamma$ , introduce non-Hermitian behavior, corresponding to the loss (for the first state) and gain (for the second state) mechanisms. This type of Hamiltonian is commonly encountered in systems exhibiting  $(\mathcal{PT})$ -symmetry, where the balance between loss and gain plays a critical role in determining the system's dynamics and phase transitions. Such models are often used in the study of open quantum systems, photonics, and systems where energy exchange with the environment is present.

The eigenvalues of  $\tilde{H}_1$  are  $\tilde{\lambda}_{\pm} = \omega_0 \pm \sqrt{g^2 - \gamma^2}$  and are real for  $g > \gamma$ . The eigenvectors  $\{|\tilde{\psi}_n\rangle, |\tilde{\phi}_n\rangle\} : \tilde{H}_1|\tilde{\psi}_n\rangle = \tilde{\lambda}_n|\tilde{\psi}_n\rangle, \tilde{H}_1^{\dagger}|\tilde{\phi}_n\rangle = \tilde{\mu}_n|\tilde{\phi}_n\rangle$  form a *biorthogonal* system [49]. In such biorthogonal systems, the metric can be constructed as [50]

$$\eta = |\tilde{\phi}_1\rangle\langle\tilde{\phi}_1| + |\tilde{\phi}_2\rangle\langle\tilde{\phi}_2| = \mathbb{1} - \frac{\gamma}{g}\sigma_y. \quad (42)$$

As expected,  $\eta \rightarrow \mathbb{1}$  as  $\gamma \rightarrow 0$ , i.e., when  $\tilde{H}_1$  approaches the Hermitian limit. By calculating the positive square root of this metric operator

$$\mathcal{E} = \sqrt{\eta} = \frac{1}{2}(\Gamma_+ + \Gamma_-)\mathbb{1} - \frac{1}{2}(\Gamma_+ - \Gamma_-)\sigma_y, \quad (43)$$

where  $\Gamma_{\pm} = \sqrt{1 \pm \frac{\gamma}{g}}$ , we obtain the Hermitian counterpart of  $\tilde{H}_1$  which is given by

$$H_1 = \mathcal{E}\tilde{H}_1\mathcal{E}^{-1} = \begin{pmatrix} \omega_0 & \sqrt{g^2 - \gamma^2} \\ \sqrt{g^2 - \gamma^2} & \omega_0 \end{pmatrix}. \quad (44)$$

Note that the eigenvalues of  $H_1$  are  $\lambda_{\pm} = \omega_0 \pm \sqrt{g^2 - \gamma^2}$  same as that of  $\tilde{H}_1$  but the eigenvectors  $|\psi_{\pm}\rangle = (\pm 1 \ 1)^T$  are *orthogonal*.

We now turn to the dynamics governed by  $\tilde{H}_1$ , where we examine the three approaches outlined in Sec. III, namely the *metric*, *time-normalization* and *master equation* approaches.

We begin with the metric formalism, where the dynamics is governed by the Hermitian counterpart of the Hamiltonian,  $\tilde{H}_1$ , as obtained in Eq. (44). This Hamiltonian evolves the qubit state in Eq. (26) as follows:

$$\rho_{\text{metric}}(t) = e^{-iHt}\rho(0)e^{iHt} = \sum_{\ell=0}^3 c_{\ell}\sigma_{\ell}, \quad (45)$$

with  $c_0 = 1/2$ ,  $c_1 = x$ ,  $c_2 = (\theta - \frac{1}{2}) \sin(2t\sqrt{g^2 - \gamma^2})$  and  $c_3 = (\theta - \frac{1}{2}) \cos(2t\sqrt{g^2 - \gamma^2})$ .

On the other hand, the time-normalization approach involves writing the Schrödinger equation for  $\tilde{H}_1$  with the solution

$$\tilde{\rho}(t) = e^{-i\tilde{H}_1 t} \tilde{\rho}(0) e^{i\tilde{H}_1^\dagger t}, \quad (46)$$

which is a trace non-preserving equation. For example, with the initial state given in Eq. (26), the trace of  $\rho_{\text{in}}$  and  $\tilde{\rho}(t)$  with respect to the *standard* metric is:

$$\begin{aligned} \text{Tr}[\rho_{\text{in}}] &= 1, \\ \text{and } \text{Tr}[\tilde{\rho}(t)] &= \frac{\gamma(2\theta - 1)}{\sqrt{g^2 - \gamma^2}} S_\beta - \frac{\gamma^2}{g^2 - \gamma^2} C_\beta + \frac{g^2}{g^2 - \gamma^2}, \end{aligned} \quad (47)$$

where  $\beta = 2t\sqrt{g^2 - \gamma^2}$ . Clearly, the trace is not preserved for any time  $t > 0$ . To make Eq. (46) physically meaningful, one may divide it by its trace, yielding the following *normalized* density matrix:

$$\tilde{\rho}_{\text{norm}}(t) = \frac{\tilde{\rho}(t)}{\text{Tr}[\tilde{\rho}(t)]}. \quad (48)$$

Note that, in the *metric* space with the metric operator given in Eq. (42), we have from Eq. (9),  $\text{Tr}[\eta\tilde{\rho}(t)] = 1$ —demonstrating the preservation of trace of  $\tilde{\rho}(t)$  in Eq. (46) in the metric space for all the evolution times and, hence, the unitary nature of dynamics. Interestingly, in this example we also have  $\text{Tr}[\eta\rho_{\text{in}}] = 1$ .

Finally, the non-Hermitian Hamiltonian Eq. (41) can be interpreted as an effective Hamiltonian emerging after neglecting the jump term in the following master equation

$$\begin{aligned} \partial_t \rho_{\text{me}}(t) &= -i[H, \rho_{\text{me}}(t)] + 2\gamma(\sigma_- \rho_{\text{me}}(t) \sigma_+ \\ &\quad - \frac{1}{2}\sigma_+ \sigma_- \rho_{\text{me}}(t) - \frac{1}{2}\rho_{\text{me}}(t) \sigma_+ \sigma_-). \end{aligned} \quad (49)$$

where  $H = \omega_0 \mathbb{1} + g\sigma_x$ . the term  $\omega_0 \mathbb{1}$  adds a constant global energy shift, which does not affect the system's dynamics, while the term  $g\sigma_x$  generates coherent oscillations (rotation around the  $x$ -axis). The system attains a steady state as  $t \rightarrow \infty$  given by

$$\rho_{\text{me,ss}} = \frac{g^2}{2(g^2 - \gamma^2)} \begin{pmatrix} 1 & -i\gamma/g \\ i\gamma/g & 1 + (\gamma/g)^2 \end{pmatrix}. \quad (50)$$

The system's dynamics under different formulations—namely, the metric-based evolution  $\rho_{\text{metric}}(t)$ , the normalized state evolution  $\tilde{\rho}_{\text{norm}}(t)$ , and the master equation solution  $\rho_{\text{me}}(t)$ —are illustrated in Fig. 4. These trajectories, shown for a representative initial state on the Bloch sphere, highlight the distinctions and similarities among the three approaches. Figure 4 (b) further provides a projection of this evolution onto the equatorial plane, offering additional geometric insight.

*Quantum Fisher Information:* To elucidate how the aforementioned approaches can yield different results in terms of

the QFI, we will examine the input state defined in Eq. (26) and concentrate on the estimation of the parameter  $\theta$ . By computing the QFI, as outlined in Eq. (22), we can quantitatively assess the effectiveness of each approach. The normalization and metric approaches respectively lead to

$$\mathcal{F}_\theta^{\text{norm}} = \frac{(g^2 - \gamma^2)^2 \mathcal{F}_\theta^{\text{metric}}}{g^2 + \gamma(2\theta - 1)\sqrt{g^2 - \gamma^2} S_\beta - \gamma^2 C_\beta}, \quad (51)$$

$$\mathcal{F}_\theta^{\text{metric}} = \frac{1 - 4x^2}{\theta(1 - \theta) - x^2}. \quad (52)$$

Thus, on one hand we have a precision (QFI) which is constant for a given value of state parameter  $x$  under metric formalism, the normalization method predicts an oscillating behavior with time. It should be noted that  $\mathcal{F}_\theta^{\text{metric}}$  in Eq. (52) is indeed the first element of QFI matrix in Eq. (29) derived for the general  $2 \times 2$  non-Hermitian Hamiltonian.

For comparison, we obtain the QFI,  $\mathcal{F}_\theta^{\text{me}}$  from the solution of the master equation in Eq. (49) and plot it in Fig. 5 along with  $\mathcal{F}_\theta^{\text{norm}}$  and  $\mathcal{F}_\theta^{\text{metric}}$  given in Eqs. 51 and 52, respectively. In the limit, where the decay rate  $\gamma \rightarrow 0$  [i.e., the Hermitian limit in Eq. (41)], all QFI measures converge to their corresponding Hermitian counterparts

$$\mathcal{F}_\theta^{\text{norm}}|_{\gamma=0} = \mathcal{F}_\theta^{\text{metric}}|_{\gamma=0} = \mathcal{F}_\theta^{\text{me}}|_{\gamma=0} = \frac{1 - 4x^2}{\theta(1 - \theta) - x^2}. \quad (53)$$

An interesting comparison arises from Eq. (51) when considering the QFI in the normalization formalism,  $\mathcal{F}_\theta^{\text{norm}}$ , and its metric counterpart,  $\mathcal{F}_\theta^{\text{metric}}$ :

$$\mathcal{F}_\theta^{\text{norm}} = \frac{1}{\text{Tr}[\tilde{\rho}(t)]^2} \mathcal{F}_\theta^{\text{metric}}. \quad (54)$$

This expression shows that the QFI in the normalization formalism is scaled by the factor  $\frac{1}{\text{Tr}[\tilde{\rho}(t)]^2}$  relative to the metric frame. Notably, when  $\text{Tr}[\tilde{\rho}(t)] < 1$ , the normalization formalism can lead to an enhancement in QFI, surpassing the Hermitian limit. This seems to imply that the normalization formalism offers a potential advantage in quantum parameter estimation when the trace of the non-Hermitian density matrix is less than unity, reflecting a *spurious* broader range of information captured by this approach.

Further, from Fig. 5 we have contrasting predictions with time about precision in measuring parameter  $\theta$ . Under the metric formalism, one can always be sure of obtaining information about parameter  $\theta$  and this information does not change over time. However, the normalization method suggests that the precision would depend on the time of measurement. In particular, one can beat the precision from metric formalism by performing measurements at  $t = 4n\pi/\sqrt{g^2 - \gamma^2}$ , for a give value of  $g$  and  $\gamma$  with  $g > \gamma$  [as already assumed above in order to ensure that the eigenvalues are real].

## B. Time-dependent metric

Next, we consider the Hamiltonian  $H = \omega\sigma_z$ , which describes the coherent evolution of the system, leading to precession about the  $z$  axis of the Bloch sphere Fig. 6 (a), and



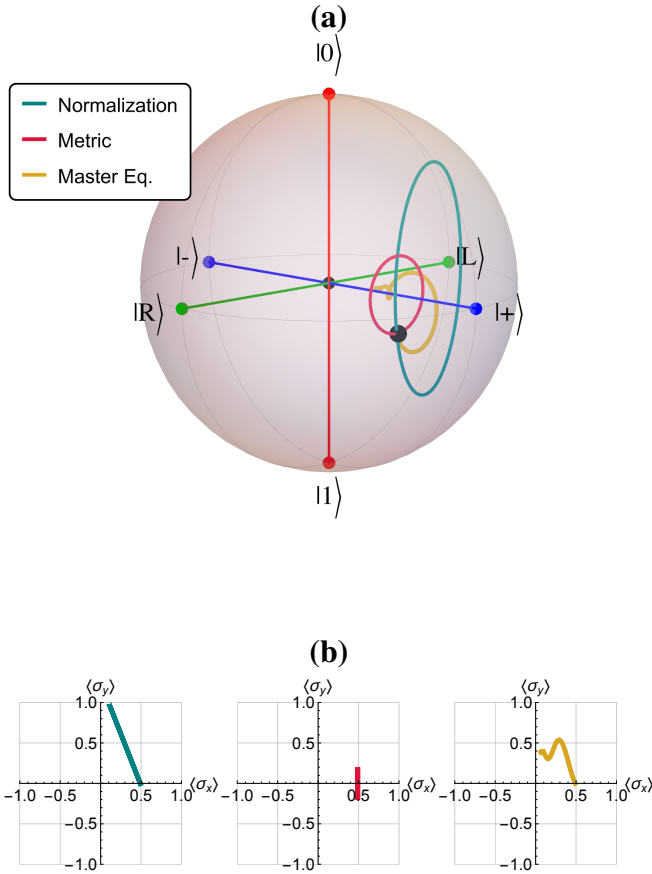


FIG. 4. **(a) Evolution of different states in the Bloch sphere:**  $\rho_{\text{metric}}(t)$  in Eq. (45), time normalized  $\tilde{\rho}_{\text{norm}}(t)$  in Eq. (48), and  $\rho_{\text{me}}(t)$  – the solution of the master equation Eq. (49). The initial state corresponds to Bloch vector  $(0.48, 0, -0.2)$  and pertains to  $\theta = 0.6$  and  $x = 0.24$  in Eq. (26). The Hamiltonian parameters used are  $g = 0.5$  and  $\gamma = 0.4$ . **(b) The evolution projected** onto the Bloch sphere equator.

the dissipation is taken into account by Lindblad operator  $L = \sqrt{\gamma}\sigma_-$ . This model captures the spontaneous emission process, where the qubit relaxes from the excited state  $|0\rangle$  to the ground state  $|1\rangle$  with a rate  $\gamma$ . This describes energy loss, such as photon emission in a two-level atom. When  $\gamma \gg \omega$ , dissipation dominates, leading to rapid relaxation and loss of coherence. For  $\gamma \ll \omega$ , coherent oscillations last longer before dissipation takes over. This balance is crucial in quantum optics and information processing for controlling decoherence. The effective Hamiltonian is given by

$$\tilde{H}_2 = H - \frac{i}{2}\Gamma^\dagger\Gamma = (\omega - i\gamma)\sigma_z, \quad (55)$$

up to a constant proportional to identity. Unlike  $\tilde{H}_1$  in Eq. (41) of the previous example, the eigenvectors of  $\tilde{H}_2$  are orthogonal, hence the method of constructing the metric for biorthogonal systems, as given in Eq. (42), does not apply. One can however obtain the metric in this case by solving Eq. (8) which yields

$$\eta(t) = 1 \cosh(2\gamma t) + \sigma_z \sinh(2\gamma t). \quad (56)$$

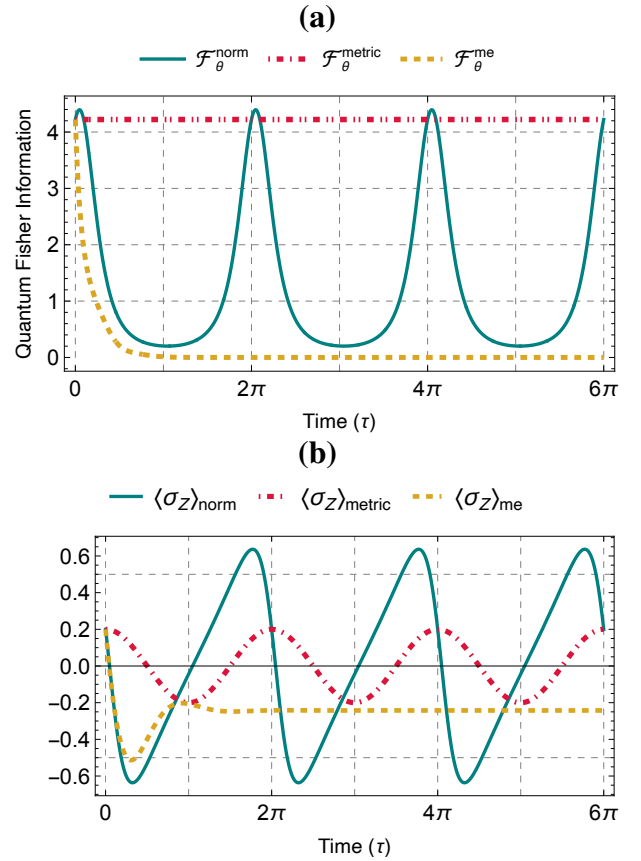


FIG. 5. **(a) QFI as a function of  $\tau = t/2\sqrt{g^2 - \gamma^2}$** , corresponding to parameter  $\theta$  as given  $\mathcal{F}_\theta^{\text{norm}}$  in Eq. (51),  $\mathcal{F}_\theta^{\text{metric}}$  in Eq. (52),  $\mathcal{F}_\theta^{\text{me}}$  for the state obtained as solution of Eq. (49) – choosing parameters  $\theta = 0.6$ ,  $x = 0.24$ ,  $g = 0.5$ ,  $\gamma = 0.4$ . **(b) Expectation value** of  $\sigma_z$  operator for different states.

This leads to the Hermitian equivalent of  $\tilde{H}_2$  given by  $H_2 = \omega_0\sigma_z$ . Without discussing the dynamics at length like in the previous section, one can similarly obtain the  $\rho_{\text{metric}}$ ,  $\tilde{\rho}_{\text{norm}}$ , and  $\rho_{\text{me}}$ .

We now consider a general observable  $A = \sum_{\ell=1}^3 a_\ell \sigma_\ell$ , with  $a_\ell = \frac{1}{2} \text{Tr}[A\sigma_\ell]$ ,  $\ell = 1, 2, 3$ . Using again the initial state Eq. (26), we obtain

$$\langle A \rangle_{\text{metric}} = (1 - 2\theta)a_3 + 2x[1 - \cos(2\omega_0 t)]a_1 + 2x \sin(2\omega_0 t)a_2, \quad (57)$$

$$\langle A \rangle_{\text{norm}} = \alpha_0 \langle A \rangle_{\text{metric}} + \alpha_1 a_3, \quad (58)$$

$$\langle A \rangle_{\text{me}} = \beta_0 \langle A \rangle_{\text{norm}} + \beta_1 a_3, \quad (59)$$

where  $\langle A \rangle_\bullet = \text{Tr}[A\rho_\bullet]$  with  $\bullet = \text{norm, metric, me}$  and

$$\alpha_0 = \frac{e^{2\gamma t}}{\theta(e^{4\gamma t} - 1) + 1} = \frac{1}{\text{Tr}[\tilde{\rho}(t)]}, \quad (60)$$

$$\alpha_1 = \frac{(e^{2\gamma t} - 1)[\theta(e^{2\gamma t} - 1) + 1]}{\theta(e^{4\gamma t} - 1) + 1}, \quad (61)$$

$$\beta_0 = \theta + (1 - \theta)e^{-4\gamma t}, \quad (62)$$

$$\beta_1 = -(1 - \theta)(1 - e^{-4\gamma t}). \quad (63)$$

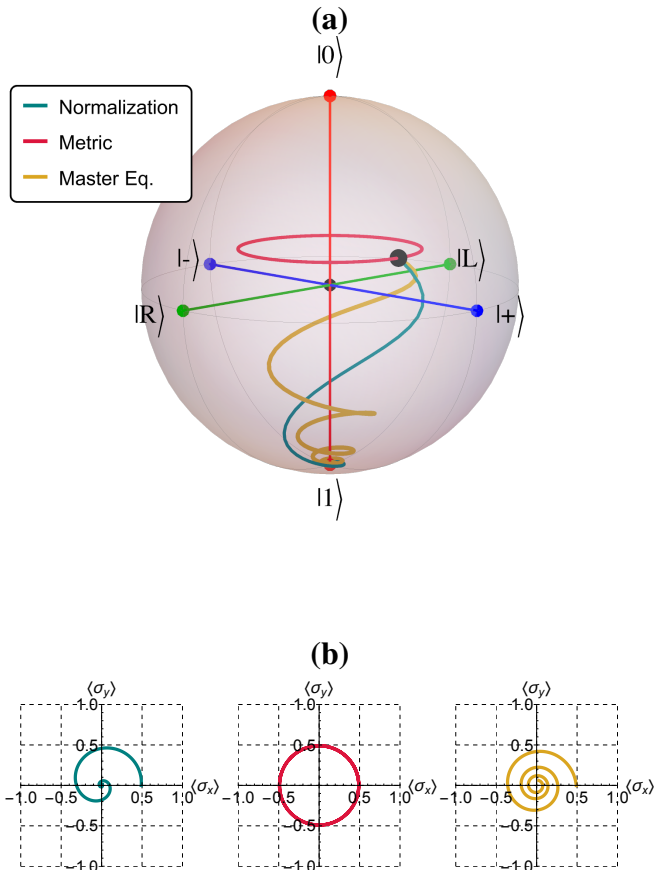


FIG. 6. **(a) Evolution of different states in the Bloch sphere:** The states shown are the same as in Fig. 4 but this time in the context of the non-Hermitian Hamiltonian given in Eq. (55). The initial state pertains to  $\theta = 0.4, x = 0.24$ . **(b) The evolution projected** onto the Bloch sphere equator.

In the long time limit, both the normalization as well as the master equation approaches show that the system settles at the ground state  $|1\rangle$ , as shown in Fig. 6, and the average of the observable  $A$  approaches the following limit

$$\lim_{t \rightarrow \infty} \langle A \rangle_{\text{norm}} = -a_3 = \lim_{t \rightarrow \infty} \langle A \rangle_{\text{me}}. \quad (64)$$

However, as expected, in the metric frame there is no such decohering effects as the system evolves under unitary dynamics. The QFI corresponding the parameter  $\theta$  follow similarly as discussed in the previous example. We obtain

$$\mathcal{F}_\theta^{\text{metric}} = \frac{1 - 4x^2}{\theta(1 - \theta) - x^2}, \quad (65)$$

$$\begin{aligned} \mathcal{F}_\theta^{\text{norm}} &= \frac{(1 - 4x^2) e^{4\gamma t}}{[\theta(1 - \theta) - x^2] [\theta(e^{4\gamma t} - 1) + 1]^2} \\ &= \frac{e^{4\gamma t}}{[\theta(e^{4\gamma t} - 1) + 1]^2} \mathcal{F}_\theta^{\text{metric}} = \frac{1}{\text{Tr}[\tilde{\rho}(t)]^2} \mathcal{F}_\theta^{\text{metric}}, \end{aligned} \quad (66)$$

$$\mathcal{F}_\theta^{\text{me}} = \frac{e^{-2\gamma t} (4x^2 - e^{2\gamma t})}{(1 - \theta)^2 + e^{2\gamma t} (\theta + x^2 - 1)}. \quad (67)$$

The metric approach once again demonstrates its effectiveness

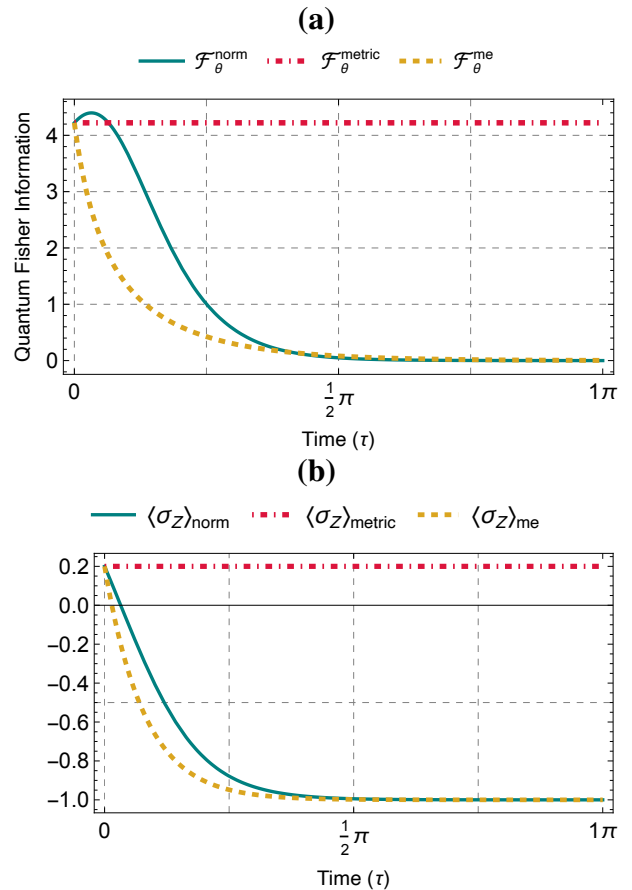


FIG. 7. **(a) QFI as a function of  $\tau = t/\gamma$**  corresponding to parameter  $\theta$  as given by  $\mathcal{F}_\theta^{\text{metric}}$  in Eq. (65),  $\mathcal{F}_\theta^{\text{norm}}$  in Eq. (66),  $\mathcal{F}_\theta^{\text{me}}$  in Eq. (67) – the state parameters chosen are  $\theta = 0.4$  and  $x = 0$ , while the Hamiltonian parameters  $g = 0.5, \gamma = 0.4$  are used. **(b) Expectation value of  $\sigma_z$  operator** for different states.

by predicting a constant, time-independent precision in quantum measurements of parameter  $\theta$ . This stability suggests that the choice of metric plays a crucial role in maintaining consistent precision over time, thereby providing a reliable framework for parameter estimation.

In contrast, the normalization method, unlike in previous example, does not exhibit any recurring behavior. But it does indicate an enhancement in precision compared to the metric (Hermitized) case for, at least, a finite initial duration. This spurious improvement implies that the normalization method may produce results that warrant further scrutiny, as its effectiveness in enhancing quantum precision may not be universally applicable.

Additionally, the master equation approach reveals a more gradual decline in the QFI over time, ultimately trending towards zero. This behavior signifies a loss of information suggesting that, as the system evolves, the ability to extract precise measurements diminishes. The gradual decrease in the QFI underscores the importance of considering different approaches when evaluating quantum precision, as each method provides distinct insights into the dynamics of the system and its associated measurement capabilities. The behavior of the QFI for the parameter  $\theta$  is shown in Fig. 7 (a), comparing

$\mathcal{F}_\theta^{\text{metric}}$ ,  $\mathcal{F}_\theta^{\text{norm}}$ , and  $\mathcal{F}_\theta^{\text{me}}$  as functions of the dimensionless time parameter  $\tau = t/\gamma$ . These results illustrate how different formulations capture the sensitivity of parameter estimation under the same initial state and Hamiltonian conditions. Figure 7(b) complements this by displaying the expectation value of the  $\sigma_z$  operator for the corresponding state evolutions, providing further dynamical insight.

Overall, these findings illustrate the nuanced differences among various approaches in predicting quantum measurement precision, emphasizing the need for careful selection of methodologies based on the specific characteristics of the quantum systems under investigation.

## VI. CONCLUSION

In summary, the comparative analysis of the metric approach, the normalization method, and the master equation framework reveals significant insights into the precision of quantum measurements. We illustrated by estimating input state parameters that the metric approach consistently predicts a constant, time-independent precision, underscoring its robustness in providing a reliable framework for analyzing quantum systems. In contrast, the normalization method, while suggesting an enhancement in precision and in some

case, a recurrent behavior with time, raises questions about the consistency of its results, warranting careful consideration in its application. The master equation approach offers a different perspective, highlighting a gradual decrease in the QFI over time, ultimately leading to a complete loss of information.

This study emphasizes the dynamic nature of quantum systems and the importance of selecting appropriate methodologies based on the specific characteristics of the system under study. Collectively, these findings underscore the necessity for a nuanced understanding of the various approaches to quantum measurement precision. Each method provides distinct insights, and their implications must be carefully evaluated to optimize the measurement capabilities in quantum metrology. Future investigations should focus on exploring the interplay between these methods and their practical applications in quantum technologies.

## ACKNOWLEDGEMENTS

This work was supported by the Polish National Science Centre (NCN) under the Maestro Grant No. DEC-2019/34/A/ST2/00081. J.K. acknowledges also the support of the National Science Centre, Poland under the SONATA BIS grant no. 2023/50/E/ST2/00457.

- 
- [1] C. W. Helstrom, “Minimum mean-squared error of estimates in quantum statistics,” *Phys. Lett. A* **25**, 101 (1967).
  - [2] D. Bures, “An extension of Kakutani’s theorem on infinite product measures to the tensor product of semifinite  $w^*$ -algebras,” *Trans. Am. Math. Soc.* **135**, 199 (1969).
  - [3] C. W. Helstrom, *Quantum Detection and Estimation Theory* (Academic Press, 1976).
  - [4] C. Helstrom, “The minimum variance of estimates in quantum signal detection,” *IEEE Transactions on Information Theory* **14**, 234 (1968).
  - [5] S. L. Braunstein and C. M. Caves, “Statistical distance and the geometry of quantum states,” *Phys. Rev. Lett.* **72**, 3439 (1994).
  - [6] S. L. Braunstein, C. M. Caves and G. J. Milburn, “Generalized uncertainty relations: Theory, examples, and lorentz invariance,” *Annals of Physics* **247**, 135 (1996).
  - [7] M. A. Ballester, “Optimal scheme for phase estimation in quantum interferometry,” *Phys. Rev. A* **70**, 032310 (2004).
  - [8] A. Monras, “Optimal phase measurements with pure Gaussian states,” *Phys. Rev. A* **73**, 033821 (2006).
  - [9] M. Aspachs, J. Calsamiglia, R. Muñoz Tapia and E. Bagan, “Phase estimation for thermal Gaussian states,” *Phys. Rev. A* **79**, 033834 (2009).
  - [10] R. Demkowicz-Dobrzański, U. Dorner, B. J. Smith, J. S. Lundeen, W. Wasilewski, K. Banaszek and I. A. Walmsley, “Quantum phase estimation with lossy interferometers,” *Phys. Rev. A* **80**, 013825 (2009).
  - [11] R. Demkowicz-Dobrzański, J. Kołodyński and M. Guţă, “The elusive Heisenberg limit in quantum-enhanced metrology,” *Nat. Commun.* **3**, 1063 (2012).
  - [12] A. W. Chin, S. F. Huelga and M. B. Plenio, “Quantum metrology in non-Markovian environments,” *Phys. Rev. Lett.* **109**, 233601 (2012).
  - [13] P. C. Humphreys, M. Barbieri, A. Datta and I. A. Walmsley, “Quantum enhanced multiple phase estimation,” *Phys. Rev. Lett.* **111**, 070403 (2013).
  - [14] N. M. Nusran and M. V. G. Dutt, “High-dynamic-range magnetometry with a single electronic spin in diamond,” *Phys. Rev. B* **90**, 024422 (2014).
  - [15] C. Sparaciari, S. Olivares and M. G. A. Paris, “Bounds to precision for quantum interferometry with Gaussian states and operations,” *J. Opt. Soc. Am. B* **32**, 1354 (2015).
  - [16] L. Pezzè, M. A. Ciampini, N. Spagnolo, P. C. Humphreys, A. Datta, I. A. Walmsley, M. Barbieri, F. Sciarrino and A. Smerzi, “Heralded phase estimation,” *Phys. Rev. Lett.* **119**, 130504 (2017).
  - [17] A. Monras and F. Illuminati, “Measurement of Gaussian states with quantum Fisher information,” *Phys. Rev. A* **83**, 012315 (2011).
  - [18] L. A. Correa, M. Mehboudi, G. Adesso and A. Sanpera, “Individual quantum probes for optimal thermometry,” *Phys. Rev. Lett.* **114**, 220405 (2015).
  - [19] G. Spedalieri, S. L. Braunstein and S. Pirandola, “Thermal quantum metrology in continuous variable systems,” *Quant. Sci. Technol.* **5**, 015008 (2019).
  - [20] P. P. Hofer, J. B. Brask, M. Perarnau-Llobet and N. Brunner, “Quantum thermometry based on energy measurements,” *Phys. Rev. Lett.* **119**, 090603 (2017).
  - [21] M. Mehboudi, M. R. Jørgensen, S. Seah, J. B. Brask, J. Kołodyński and M. Perarnau-Llobet, “Fundamental limits in Bayesian thermometry and attainability via adaptive strategies,” *Phys. Rev. Lett.* **128**, 130502 (2022).

- [22] W. Wasilewski, K. Jensen, H. Krauter, J. J. Renema, M. V. Balabas and E. S. Polzik, “Quantum noise limited and entanglement-assisted magnetometry,” *Phys. Rev. Lett.* **104**, 133601 (2010).
- [23] J. Cai and M. B. Plenio, “Large-scale quantum sensing with a single spin,” *Phys. Rev. Lett.* **111**, 230503 (2013).
- [24] Y.-L. Zhang, H. Wang, L. Jing, L.-Z. Mu and H. Fan, “Quantum metrology with state-independent multipartite entanglement,” *Sci. Rep.* **4**, 7390 (2014).
- [25] R. Nair and M. Tsang, “Quantum estimation of the separation between two incoherent point sources,” *Phys. Rev. Lett.* **117**, 190801 (2016).
- [26] J. Amorós-Binefa and J. Kołodyński, “Noisy atomic magnetometry in real time,” *N. J. Phys.* **23**, 123030 (2021).
- [27] R. Gaiba and M. G. A. Paris, “Squeezing and quantum Fisher information of Gaussian states,” *Phys. Lett. A* **373**, 934 (2009).
- [28] D. Šafránek and I. Fuentes, “Estimation of Gaussian quantum states,” *Phys. Rev. A* **94**, 062313 (2016).
- [29] L. Pezzé and A. Smerzi, “Entanglement, nonlinear dynamics, and the Heisenberg limit,” *Phys. Rev. Lett.* **102**, 100401 (2009).
- [30] G. Tóth, “Multipartite entanglement and high-precision metrology,” *Phys. Rev. A* **85**, 022322 (2012).
- [31] X.-M. Lu, X. Wang and C. P. Sun, “Quantum Fisher information flow and non-Markovian processes of open systems,” *Phys. Rev. A* **82**, 042103 (2010).
- [32] M. M. Taddei, B. M. Escher, L. Davidovich and R. L. de Matos Filho, “Quantum speed limit for physical processes,” *Phys. Rev. Lett.* **110**, 050402 (2013).
- [33] A. Smerzi, “Entanglement, nonlinear dynamics, and the Heisenberg limit,” *Phys. Rev. Lett.* **109**, 150410 (2012).
- [34] F. Schäfer, I. Herrera, S. Cherukattil, C. Lovecchio, F. S. Cataliotti, F. Caruso and A. Smerzi, “Experimental realization of quantum Zeno dynamics,” *Nat. Comm.* **5**, 3194 (2014).
- [35] F. Fröwis and W. Dür, “Are closer macroscopic quantum states less distinguishable?” *Phys. Rev. Lett.* **106**, 110402 (2011).
- [36] Ş. K. Özdemir, S. Rotter, F. Nori and L. Yang, “Parity–time symmetry and exceptional points in photonics,” *Nat. Materials* **18**, 783 (2019).
- [37] R. El-Ganainy, K. G. Makris, M. Khajavikhan, Z. H. Musslimani, S. Rotter and D. N. Christodoulides, “Non-Hermitian physics and PT symmetry,” *Nat. Phys.* **14**, 11 (2018).
- [38] M. Parto, Y. G. N. Liu, B. Bahari, M. Khajavikhan and D. N. Christodoulides, “Non-Hermitian and topological photonics: optics at an exceptional point,” *Nanophotonics* **10**, 403 (2021).
- [39] W. D. Heiss, “The physics of exceptional points,” *J. Phys. A: Math. Theor.* **45**, 444016 (2012).
- [40] C. L. Degen, F. Reinhard and P. Cappellaro, “Quantum sensing,” *Rev. Mod. Phys.* **89**, 035002 (2017).
- [41] J. Wiersig, “Enhancing the sensitivity of frequency and energy splitting detection by using exceptional points: Application to microcavity sensors for single-particle detection,” *Phys. Rev. Lett.* **112**, 203901 (2014).
- [42] J. Wiersig, “Enhancing the sensitivity of frequency and energy splitting detection by using exceptional points: Application to microcavity sensors for single-particle detection,” *Phys. Rev. A* **101**, 053846 (2020).
- [43] W. Chen, S. K. Ozdemir, G. Zhao, J. Wiersig and L. Yang, “Exceptional points enhance sensing in an optical microcavity,” *Nature* **548**, 192 (2017).
- [44] H.-K. Lau and A. A. Clerk, “Fundamental limits and non-reciprocal approaches in non-Hermitian quantum sensing,” *Nat. Commun.* **9**, 1 (2018).
- [45] C. Chen, L. Jin and R.-B. Liu, “Sensitivity of parameter estimation near the exceptional point of a non-Hermitian system,” *N. J. Phys.* **21**, 083002 (2019).
- [46] X. Zhang, Y. Chen and H. Wu, “Quantum Fisher information near exceptional points in open quantum systems,” *Phys. Rev. A* **102**, 033509 (2020).
- [47] J. Naikoo, R. W. Chhajlany and J. Kołodyński, “Multiparameter estimation perspective on non-Hermitian singularity-enhanced sensing,” *Phys. Rev. Lett.* **131**, 220801 (2023).
- [48] J. Naikoo, R. W. Chhajlany and A. Miranowicz, “Enhanced quantum sensing with hybrid exceptional-diabolic singularities,” *New J. Phys.* **27**, 064505 (2025).
- [49] D. C. Brody, “Biorthogonal quantum mechanics,” *J. Phys. A: Math. Theor.* **47**, 035305 (2013).
- [50] A. Mostafazadeh, “Pseudo-Hermitian Representation of Quantum Mechanics,” *International Journal of Geometric Methods in Modern Physics* **7**, 1191 (2002).
- [51] A. Mostafazadeh, “Metric operators for quasi-Hermitian Hamiltonians and the equivalence of quantum systems,” *J. Phys. A: Math. Theor.* **43**, 244020 (2010).
- [52] Y. Chu, Y. Liu, H. Liu and J. Cai, “Quantum sensing with a single-qubit pseudo-Hermitian system,” *Phys. Rev. Lett.* **124**, 020501 (2020).
- [53] L. Xiao, Y. Chu, Q. Lin, H. Lin, W. Yi, J. Cai and P. Xue, “Non-Hermitian sensing in the absence of exceptional points,” *Phys. Rev. Lett.* **133**, 180801 (2024).
- [54] X. Yu and C. Zhang, “Quantum parameter estimation of non-Hermitian systems with optimal measurements,” *Phys. Rev. A* **108**, 022215 (2023).
- [55] X. Yu, X. Zhao, L. Li, X.-M. Hu, X. Duan, H. Yuan and C. Zhang, “Toward Heisenberg scaling in non-Hermitian metrology at the quantum regime,” *Science Advances* **10**, eadk7616 (2024).
- [56] S. Tanaka and N. Yamamoto, “Information amplification via postselection: A parameter-estimation perspective,” *Phys. Rev. A* **88**, 042116 (2013).
- [57] J. Combes, C. Ferrie, Z. Jiang and C. M. Caves, “Quantum limits on postselected, probabilistic quantum metrology,” *Phys. Rev. A* **89**, 052117 (2014).
- [58] A. Mostafazadeh, “Pseudo-Hermiticity versus PT-symmetry ii. A complete characterization of non-Hermitian Hamiltonians with a real spectrum,” *J. Math. Phys.* **43**, 2814–2816 (2002).
- [59] C.-Y. Ju, A. Miranowicz, F. Minganti, C.-T. Chan, G.-Y. Chen and F. Nori, “Einstein’s quantum elevator: Hermitization of non-Hermitian Hamiltonians via a generalized vielbein formalism,” *Phys. Rev. Res.* **4**, 023070 (2022).
- [60] C.-Y. Ju, A. Miranowicz, J. Barnett, G.-Y. Chen and F. Nori, “Heisenberg and Heisenberg-like representations via Hilbert-space-bundle geometry in the non-Hermitian regime,” *Phys. Rev. A* **111**, 052213 (2025).
- [61] A. Mostafazadeh, “Time-dependent pseudo-Hermitian Hamiltonians and a hidden geometric aspect of quantum mechanics,” *Entropy* **22**, 471 (2020).
- [62] D. C. Brody and E.-M. Graefe, “Mixed-state evolution in the presence of gain and loss,” *Phys. Rev. Lett.* **109**, 230405 (2012).
- [63] W. H. Louisell, *Quantum Statistical Properties of Radiation* (Wiley, New York, 1973).
- [64] C.-Y. Ju, A. Miranowicz, G.-Y. Chen and F. Nori, “Non-Hermitian Hamiltonians and no-go theorems in quantum information,” *Phys. Rev. A* **100**, 062118 (2019).
- [65] C. M. Bender, D. C. Brody, H. F. Jones and B. K. Meister, “Faster than Hermitian quantum mechanics,” *Phys. Rev. Lett.* **98**, 040403 (2007).
- [66] A. Mostafazadeh, “Quantum brachistochrone problem and the geometry of the state space in pseudo-Hermitian quantum mechanics,” *Phys. Rev. Lett.* **99**, 130502 (2007).

- [67] K. Sim, N. Defenu, P. Mognini and R. Chitra, “Quantum metric unveils defect freezing in non-Hermitian systems,” *Phys. Rev. Lett.* **131**, 156501 (2023).
- [68] J. J. Peřina Jr., A. Miranowicz, G. Chimczak and A. Kowalewska-Kudłaszyk, “Quantum Liouvillian exceptional and diabolical points for bosonic fields with quadratic Hamiltonians: The Heisenberg-Langevin equation approach,” *Quantum* **6**, 883 (2022).
- [69] J. Peřina, A. Miranowicz, J. K. Kalaga and W. Leoński, “Unavoidability of nonclassicality loss in  $\mathcal{PT}$ -symmetric systems,” *Phys. Rev. A* **108**, 033512 (2023).
- [70] R. Wakefield, A. Laing and Y. N. Joglekar, “Non-Hermiticity in quantum nonlinear optics through symplectic transformations,” *Appl. Phys. Lett.* **124**, 201103 (2024).
- [71] J. Peřina Jr., K. Thapliyal, G. Chimczak, A. Kowalewska-Kudłaszyk and A. Miranowicz, “Multiple quantum exceptional, diabolical, and hybrid points in multimode bosonic systems: II. Nonconventional  $\mathcal{PT}$ -symmetric dynamics and unidirectional coupling,” e-print arXiv:2405.01667 [quant-ph].
- [72] K. Thapliyal, J. P. Jr., G. Chimczak, A. Kowalewska-Kudłaszyk and A. Miranowicz, “Multiple quantum exceptional, diabolical, and hybrid points in multimode bosonic systems: I. Inherited and genuine singularities,” e-print arXiv:2405.01666 [quant-ph].
- [73] S. M. Kay, *Fundamentals of statistical signal processing: estimation theory* (Prentice-Hall, 1993).
- [74] R. Demkowicz-Dobrzański, W. Górecki and M. Guřa, “Multi-parameter estimation beyond quantum Fisher information,” *J. Phys. Math. Theor.* **53**, 363001 (2020).
- [75] S. Luo and Q. Zhang, “Informational distance on quantum-state space,” *Phys. Rev. A* **69**, 032106 (2004).
- [76] W. Zhong, Z. Sun, J. Ma, X. Wang and F. Nori, “Fisher information under decoherence in Bloch representation,” *Phys. Rev. A* **87**, 022337 (2013).
- [77] A. Mostafazadeh, “Exact  $\mathcal{PT}$ -symmetry is equivalent to Hermiticity,” *J. Phys. A: Math. Gen.* **36**, 7081–7091 (2003).
- [78] Y. Ma, M. Pang, L. Chen and W. Yang, “Improving quantum parameter estimation by monitoring quantum trajectories,” *Phys. Rev. A* **99**, 032347 (2019).